Published in final edited form as:
Soft Matter. 2011 January 1; 2011(7): 3228–3233. doi:10.1039/C0SM01157F.

Shear thickening of F-actin networks crosslinked with non-muscle myosin IIB

Melanie Norstrom[a] and **Margaret L. Gardel**[*,a,b]

[a]Institute for Biophysical Dynamics, University of Chicago, Gordon Center for Integrative Science, E233, 929 E 57th St, Chicago, IL, 60637, USA

[b]James Franck Institute and Physics Department, University of Chicago, Chicago, IL, 60637, USA

Abstract

The material properties of cytoskeletal F-actin networks facilitate a broad range of cellular behaviors, whereby in some situations cell shape is preserved in the presence of force and, at other times, force results in irreversible shape change. These behaviors strongly suggest that F-actin networks can variably deform elastically or viscously. While a significant amount is known about the regulation of the elastic stiffness of F-actin networks, our understanding of the regulation of viscous behaviors of F-actin networks is largely lacking. Here, we study the rheological behavior of F-actin networks formed with heavy meromyosin non-muscle IIB (NMMIIB). We show that NMMIIB quenched with ADP crosslinks F-actin into networks that, for sufficient densities, display stress stiffening behavior. By performing a series of creep tests, we show that densely crosslinked actin/NMMIIB–ADP networks undergo viscous deformation over a wide range of stresses, ranging from 0.001 to 10 Pa. At high stresses, networks that stress stiffen are also observed to shear thicken, whereby the effective viscosity increases as a function of stress. Shear thickening results in a reduction in the extent of irreversible, viscous deformation in actin/NMMIIB–ADP networks at high stresses compared to that expected for a linear viscoelastic material. Thus, viscous deformation contributes less to the overall mechanical response at high levels of applied force. Our results indicate mechanisms by which the fluid-like nature of the actomyosin cytoskeleton can be reduced under high load.

1 Introduction

The actin cytoskeleton plays an essential role in numerous physical behaviors of animal cells including mediating shape changes during cell division and migration and maintaining a stable shape in response to external forces.[1,2] These diverse physical behaviors strongly suggest that the actin cytoskeleton can variably behave either fluid-like, to accommodate structural rearrangements, or solid-like, to preserve shape. The mechanical behaviors of the actin cytoskeleton are largely determined by a myriad of actin-binding proteins, to regulate the assembly of actin into dynamic, force-generating networks and bundles.[3] In non-muscle cells, non-muscle myosin II motors play essential roles in building contractile actin networks and bundles that support both movement, or flow, of the actin cytoskeleton and provide an elastic framework for cytoskeletal force transmission.[4,5] Thus, understanding the viscoelastic behaviors of the actomyosin cytoskeleton is essential for an understanding of cell mechanics.

[*]gardel@uchicago.edu; Fax: +1 773-834-0406; Tel: +1 773-834-5871.

In the presence of permanent and incompliant crosslinking proteins, F-actin networks form soft elastic gels with a well-defined, zero frequency plateau modulus that is sharply sensitive to small variations in the F-actin concentration and crosslink density.[6,7] Due to non-linearity in the entropic spring constant of the semi-flexible F-actin at high extensions, the magnitude of the elastic modulus increases at high stresses, a phenomenon known as stress stiffening.[6–8] Permanently crosslinked F-actin networks are elastic at long time scales; in the presence of a constant applied stress, the networks deform to a certain strain but no significant change in the strain, or creep, is observed and the strain recovers quickly to zero after the stress is removed.[9] Thus, while the elastic response of permanently crosslinked F-actin networks is well understood, these studies do not explore the viscous behaviors of the actin cytoskeleton.

Nearly all physiological F-actin binding proteins have a finite binding affinity to actin, which facilitates dynamic crosslinks between F-actins. Previous studies on the rheology of dynamically crosslinked F-actin networks have focused primarily on the elastic response of F-actin networks formed with heavy meromyosin skeletal muscle II[10–12] and α-actinin.[13–15] The contributions of thermalized unbinding of transient crosslinks can capture the frequency dependent, linear viscoelastic properties of these actin networks.[10,15] However, the extent to which non-linear effects occur in the viscous behavior of transiently cross-linked F-actin networks is unknown.

Here, we measure the stress-dependent viscoelasticity in an *in vitro* model of the actomyosin cortex of non-muscle cells comprised of a network of F-actin crosslinked with heavy meromyosin non-muscle IIB (NMMIIB). We show that NMMIIB saturated with ADP, to promote a high affinity to actin, can efficiently crosslink F-actin into viscoelastic networks. The elastic properties are similar to those observed previously with moderate stress stiffening observed in densely crosslinked networks. Here, we demonstrate that these networks also exhibit shear thickening, whereby the effective viscosity increases by over ten-fold as the applied stress increased from 0.01 to 4 Pa. This increased viscosity is a result of both increased elastic modulus and stress relaxation time at high stresses. A significant consequence of shear thickening is that the extent of irreversible, viscous deformation of the networks saturates at high stresses. Consequently, we find that the relative contribution of viscous deformations of the network is reduced under applied load. These results have significant implications for the role of applied stresses in the modulation of the fluid-like behaviors of the actomyosin cytoskeleton.

2 Experimental procedures

2.1 Protein preparation

Heavy meromyosin non-muscle IIB is prepared as previously described[16] and consists of dimeric constructs of non-muscle myosin IIB containing two enzymatically active heads. Myosin activity is confirmed using a gliding filament assay.[16] Actin is prepared from acetone powder as previously described and is stored in G-buffer (2 mM Tris–HCl, 0.2 mM $CaCl_2$, 0.2 mM ATP, 0.2 mM β-mercaptoethanol and 0.01% Na–azide).[17] All samples contain either 2 mM ADP or 2 mM ATP (Calbiochem), which we previously determined to be saturating concentrations of nucleotide. In the presence of saturating ADP, the release of myosin heads from actin is inhibited.[18] Saturating ATP shortens the myosin dwell time on actin by causing the catalytic heads to cycle and release from the actin at their maximal rate.[16,19]

2.2 Rheology

Rheological experiments are performed on a Bohlin Gemini HRnano (Malvern Instruments) using a 40 mm acrylic plate and 100 μm gap. Experiments are performed in F-actin polymerization buffer containing 25 mM KCl, 25 mM imidazole–HCl pH 7.5, 1 mM EGTA, 4 mM $MgCl_2$ and 1 mM DTT. To form isotropic networks, nucleotide, myosin and G-actin are added sequentially to F-buffer at appropriate concentrations. After mixing, the solution is placed on the sample plate and incubated for 1 hour before measurements were made. Network polymerization is assessed by monitoring the elastic modulus for five minutes at a single frequency to confirm that no change in the modulus is observed. Effects of ATP depletion are not observed over a 3 hour measurement window.

3 Results and discussion

3.1 Non-muscle myosin IIB crosslinks actin when saturated with ADP

To serve as a mimimal model of the actomyosin cortex in non-muscle cells, we chose to form networks of F-actin crosslinked with heavy meromyosin non-muscle IIB (NMMIIB) motors (Fig. 1). Full length non-muscle myosin IIB is widely expressed in non-muscle cells, with important roles in establishing cell polarity, cell division and cell adhesion.[4,5] Similar to other myosin motors, NMMIIB undergoes a mechanochemical cycle in the presence of ATP that facilitates both translocation of F-actin and force generation within the actomyosin bond. Within this cycle, NMMIIB has a weak affinity to F-actin when complexed with ATP ($k_{off} \approx 1\ s^{-1}$)[16] and a significantly higher affinity when complexed with ADP ($k_{off} \approx 0.0003\ s^{-1}$).[19] The binding affinity between F-actin and ADP–myosin shows rich force-dependence which can lead to enhanced lifetimes under applied load.[20] Within cells, full-length non-muscle myosin IIB assembles into minifilaments comprised of ~20 myosin motors.[21] To isolate the mechanical impact of the actomyosin bond and minimize the effect of structural rearrangements that can occur with the filamentous myosin,[22,23] we chose to work with heavy meromyosin non-muscle IIB (NMMIIB), which assembles into dimers.

To characterize the extent to which NMMIIB can cross-link F-actin into networks, 10 μmM G-actin is polymerized in the presence of a variety of concentrations of NMMIIB, ranging from 0 to 1 μM, such that the molar ratio of NMMIIB to G-actin, R, varies from 0 to 0.1. We form networks either in the presence of 2 mM ATP, to facilitate the mechanochemical cycle of myosin, or 2 mM ADP, which engages myosin into a high affinity binding state to F-actin. Since we polymerize F-actin in the absence of regulatory proteins, we expect the mean F-actin length to be 7–10 μm,[24] significantly larger than the expected mesh size of the network, $\xi \approx 0.5$ μm.[25]

The rheological effects of NMMIIB crosslinking are observed when actin/NMMIIB networks form in the presence of 2 mM ADP. The elastic modulus for actin/NMMIIB–ADP networks is constant between 1 and 0.01 Hz and is over 10-fold greater than the magnitude of the viscous modulus (Fig. 2a); we denote the value of the elastic modulus measured at 0.2 Hz as $G'_{0.2}$. $G'_{0.2}$ is highly dependent on the NMMIIB concentration, increasing from 0.3 Pa to 1.5 Pa between $R = 0.001$ and 0.1 (Fig. 2b, closed circles). These characteristics indicate that NMMIIB–ADP can efficiently crosslink F-actin into predominately elastic networks. While previous electron microscopy data have speculated this crosslinking capability of NMMIIB,[18] this is the first rheological data showing the impact on the network elasticity.

Around 0.1 Hz, we observe a weak local minimum in the viscous modulus of the actin/NMMIIB–ADP networks. Previous measurements of networks formed with the heavy meromyosin skeletal muscle II (SkMM–ADP) observed a similar minimum, albeit at higher frequencies, around 1 Hz.[10,11] However, by contrast to these earlier measurements, we observe no decrease in the elastic modulus down to frequencies of 0.001 Hz. This suggests

that relaxation time scales for actin/NMMIIB–ADP networks, as measured by the linear viscoelastic response, are significantly longer than those of actin/SkMM–ADP networks.

In the presence of 2 mM ATP, NMMIIB does not significantly alter the viscoelasticity of actin/NMMIIB–ATP networks from that of entangled F-actin. The magnitude of $G'_{0.2}$ is similar to that observed for entangled F-actin and insensitive to changes in the concentration of NMMIIB–ATP as R varies from 0.001 to 0.1 (Fig. 2b, open circles). These results are consistent with previous rheological measurements of F-actin networks formed in the presence of heavy meromyosin skeletal muscle quenched with ATP[26,27] and are also consistent with the idea that, in the presence of ATP, the short-lived interactions of cycling myosin heads[16,19,28] diminish the capability of myosin dimers to efficiently crosslink F-actin.

3.2 Actin networks crosslinked with NMMIIB–ADP creep

To measure the viscoelastic behavior under different levels of applied stress, a series of creep and creep recovery tests are performed (Fig. 3a and b). Here, a constant stress is applied for 30 seconds and then removed while the strain is continuously monitored. These creep and creep recovery measurements are then repeated for a range of stresses, ranging from 0.001 to 4.0 Pa. For applied stresses as low as 0.01 Pa, entangled F-actin solutions demonstrate considerable creep, with the strain increasing from 0.05 to 0.12 within 30 seconds of applied stress (Fig. 3a). This is consistent with previous results,[9] and likely arises from the transient nature of physical entanglements in F-actin solutions.

Despite the strong crosslinking effects observed in the linear viscoelastic response, creep is also observed in actin/NMMIIB–ADP networks when a steady stress is applied for 30 s. For relatively low stresses, on the order of 0.1 Pa, the strain increases from 0.06 to 0.08 whereas, at a higher stress of 1 Pa, the strain increases from 0.33 to 0.41 (Fig. 3b). Thus, the transient nature of the NMMIIB–ADP crosslinking is apparent even at short time scales in these creep measurements.

3.3 Densely crosslinked actin/NMMIIB–ADP networks stress stiffen

From the series of creep tests, we examine relationships between stress and strain or strain rate over a wide range of applied stress, σ_0. The ratio of σ_0 to the average strain measured between 15 and 30 s, γ_{avg}, provides a measure of the effective elastic modulus during the creep measurement, $G'_{eff} = \sigma_0/\gamma_{avg}$.

For entangled F-actin solutions, G'_{eff} is constant for applied stresses below 0.1, indicative of linear elastic behavior (Fig. 3c, squares). By contrast, as the applied stress is increased above 0.1 Pa, G'_{eff} decreases, indicating stress weakening behavior which is known to occur for F-actin solutions.[7] Sparsely crosslinked actin/NMMIIB–ADP networks ($R = 0.025$) also have a constant G'_{eff} for stresses up to 0.1 Pa, but show slight stress stiffening behavior, with G'_{eff} increasing from 0.3 to 0.45 Pa as the applied stress is increased from 0.1 to 1 Pa (Fig. 3c, circles).

By contrast, densely crosslinked actin–NMMIIB–ADP networks ($R = 0.05$) show significant stress stiffening above applied stresses of 0.1 Pa (Fig. 3c, triangles). When $\sigma_0 < 0.1$, G'_{eff} is remarkably constant. However, when σ_0 is greater than 0.1 Pa, G'_{eff} increases from 1.5 to 5 Pa. These results are consistent with previously known transitions between stress weakening and stress stiffening behavior as the crosslink density is increased.[7] Furthermore, they are qualitatively consistent with other types of measurements used to assess the non-linear elastic response.[9]

3.4 Stress stiffening networks demonstrate higher effective viscosity at higher stresses

To further evaluate the changes in the viscoelastic nature of the networks under applied stress, we calculate the effective viscosity, η_{eff}, by determining the ratio between the applied stress, σ_0, to the strain rate during the creep measurement. The strain rate is calculated by finding the difference in strain between 5 and 30 s and dividing by the time to obtain, $\gamma = (\gamma(30\ s) - \gamma(5\ s)/25$ s. For entangled F-actin solutions, η_{eff} is approximately 10 Pa s and independent of the applied stress below 0.1 Pa, (Fig. 4a, squares). At stresses larger than 0.1 Pa, η_{eff} decreases, consistent with large deformation rates that occur prior to breaking. For networks which are weakly stress stiffening ($R = 0.025$), the effective viscosity is remarkably constant between 0.01 and 1 Pa (Fig. 4a, open circles).

For densely crosslinked samples, the effective viscosity increases moderately, from 10 Pa s to 30 Pa s as the applied stress is increased from 0.001 Pa to 0.1 Pa. At stresses above 0.3 Pa, the effective viscosity increases sharply, from 30 Pa s to nearly 1000 Pa s as the stress is increased up to 4 Pa (Fig. 4a, triangles). Thus, the effective viscosity is proportional to the applied stress, $\eta_{eff} \approx \sigma_0$, and indicates that the viscosity is strongly divergent at a critical strain rate. Thus, densely crosslinked actin/NMMIIB–ADP networks demonstrate significant shear thickening whereby the effective viscosity increases as a function of applied stress.

In a simplified Maxwell model, the viscosity is equal to the product of the elastic modulus and a time constant characterizing the stress relaxation, τ, such that: $\eta \approx G'\tau$. Thus, samples that have stress-dependent changes in G' would be expected to yield stress-dependent changes in η without any changes to τ. However, by calculating $\tau = \eta_{eff}/G'_{eff}$, we find that s is not constant but rather increases from 10 s to nearly 100 s as the applied stress is increased from 0.01 to 4 Pa (Fig. 4b, triangles). Thus, the increase in the effective viscosity at high stresses likely occurs, in part, from both the increased elastic modulus at high stresses as well as increased stress relaxation time scales.

3.5 Shear thickening samples preserve shape at high stresses

A second metric by which to characterize the viscous, irreversible flow is to determine the extent to which the materials regain their shape after the applied stress is removed during the creep recovery phase. For a perfectly elastic sample, the strain quickly returns back to zero after removal of the applied stress whereas for a purely viscous material, the strain remains unchanged. Thus, the extent of the unrecovered strain, measured by the difference between the strain measured at the end of the creep recovery and the strain prior to application of the applied stress, characterizes the extent of viscous flow of the network.

The total sample deformation can be deconstructed into the sum of two modes of deformation reflecting the reversible, elastic deformation, γ_e, and the irreversible, viscous deformation, γ_v, such that $\gamma = \gamma_e + \gamma_v$. If the strains are additive, the total applied stress, σ_0, is equal to both the stress resulting in viscous deformation, σ_v, and the stress resulting in elastic deformation, σ_e, such that: $\sigma_0 = \sigma_e = \sigma_v$.[9] For a sample with a constant viscosity, then $\gamma_v \approx \sigma_0$ and the unrecoverable strain should be linear with the magnitude of applied stress.

Both entangled F-actin solutions and actin/NMMIIB–ADP networks show incomplete recovery of strain, consistent with an irrecoverable viscous flow. For entangled F-actin solutions, the unrecovered strain increases linearly with applied stresses below 0.08 Pa (Fig. 4c, solid squares). At higher stresses, the unrecovered strain increases faster than the changes in the stress, consistent with the decreased effective viscosity shown in Fig. 4a. The unrecovered strain in weakly crosslinked actin/NMMIIB–ADP networks varies linearly with the applied stress over the entire range of measurement, from 0.008 to 0.8 Pa s (Fig. 4c, open circles).

For densely crosslinked actin/NMMIIB–ADP networks (R = 0.05), the extent of the unrecovered strain increases linearly with an applied stress below 0.1 Pa, consistent with the constant effective viscosity over this range (Fig. 4c, closed triangles). However, at higher stresses, the unrecovered strain approaches a plateau such that increased stress does not result in higher amounts of the unrecovered strain. Thus, shear thickening samples have enhanced shape preservation at higher stresses than one would expect for linear viscoelastic samples.

3.6 Densely crosslinked actomyosin networks become more elastic at high stresses

The nature of the viscous relaxation in actin networks formed with transient crosslinkers is likely to arise from numerous processes involving a broad spectrum of relaxation time scales.[15] Indeed, during a 30 s creep experiment, we observe that the strain resembles a power law, such that $\gamma(t) \approx \gamma_0 t^{\alpha}$ (Fig. 5a). Similar power law behavior is observed for creep measurements over much longer times, on the order of 30 min (data not shown). The magnitude of α reflects the viscoelastic nature of the network, with α = 0 reflective of a pure elastic solid and α = 1 reflecting a viscous fluid. For stresses between 0.001 and 0.01 Pa, entangled F-actin solutions and actin/NMMIIB–ADP networks have similar values of α, approximately 0.12 (Fig. 5b). For stresses above 0.04, α begins to increase for solutions of entangled F-actin, a further indication of the fluidization of these networks at higher stresses (Fig. 5b, squares). By contrast, as stresses are increased from 0.01 to 1 Pa, α decreases for actin/NMMIIB–ADP networks, reflecting the solidification of these networks at higher stresses (Fig. 5b, triangles). Interestingly, at higher stresses, α begins to increase again prior to network breaking. Thus, under a range of increased stresses, actin/NMMIIB–ADP networks behave more solid-like.

4 Conclusions

Here we have explored the viscoelastic properties of F-actin networks formed with heavy meromyosin non-muscle IIB. Similar to what has been found for heavy meromyosin skeletal muscle II (SkMM),[10–12] heavy meromyosin non-muscle IIB can efficiently crosslink F-actin into elastic networks when quenched in the high affinity ADP-binding state. Interestingly, the linear viscoelasticity of actin/NMMIIB–ADP networks has striking differences from actin/SkMM–ADP networks that may reflect differences in the nature of these two crosslinkers. For similar network compositions, actin/NMMIIB–ADP networks appear to have a lower elastic modulus, suggesting that the efficiency of crosslinking by NMMIIB–ADP may be impaired. Furthermore, the viscous relaxation time scales of the actin/SkMM–ADP occur within 0.1–1 Hz; by contrast, no such relaxation is observed for actin/NMMIIB–ADP networks down to 0.001 Hz. These results are consistent with the higher affinity of NMMIIB–ADP to actin,[19,29] which is speculated to be important for the contribution of NMMIIB in maintaining cellular tension.[30]

By performing a series of creep measurements over a range of stresses, we characterized the viscoelastic nature of the actin/NMMIIB-ADP networks at different levels of force. Similar to previous data for densely crosslinked F-actin networks, we observe stress stiffening at high concentrations of NMMIIB–ADP. However, we also identify that these networks also shear thicken, such that the effective viscosity also increases under high stresses. The consequence of a stress-dependent viscosity is that the extent of unrecoverable deformation is not linearly proportional to applied stress, as one would expect for a linear visco-elastic material. The net result is that these networks behave more solid like at higher stresses, such that the extent of irreversible, viscous flow is diminished.

One possible mechanism for enhanced solid-like behavior at high stress is an increased time scale of actomyosin crosslinks. Numerous reports have shown that the binding affinity of

myosin motors to actin increases under tensile load.[16,31] Importantly, the bond between actin and ADP–myosin, as is studied here, has been shown to behave as a catch bond, whereby the bond affinity increases with applied force, for forces up to 5 pN.[20] At even higher forces, a transition to slip bond behavior, whereby the bond affinity decreases with applied force, is observed. We can estimate the force on individual actin/ADP–myosin bonds in our experiments by considering the length scale between effective crosslinks within our network, $\xi \approx 0.5$ μm. By multiplying the applied stress by $\xi^2 \approx 0.25$ μm^2, the forces applied to each dimer can be estimated to range from 0.25 pN to 2.5 pN as the applied stress is increased from 1 Pa to 10 Pa. Thus, the stresses we are applying at the macroscopic scale are consistent with the range of forces where individual actin/ADP–myosin bonds are expected to display catch bond behavior. Consistent with slip bond behavior at even higher loads, stresses higher than 10 Pa cannot be sustained by our reconstituted actomyosin networks. Thus, our results suggest rheological consequences of single molecule behavior on viscous flows within actomyosin networks at different levels of tension.

Recent data have shown that the extent of viscous flow of actomyosin networks within cells is force-dependent. Nearly all adherent cells demonstrate a “retrograde” flow of actomyosin networks from the cell periphery towards the cell nucleus.[32] Recently, work has shown that the rate of flow decreases as the tension within the actomyosin network increases.[33] Our data indicate that these observations in live cells could reflect shear thickening of the actomyosin networks, such that stress relaxation time scales increase at higher amounts of tension. This mechanism would facilitate large scale, rapid rearrangements and deformations of the actomyosin cytoskeleton at low tension, but facilitate efficient stress transmission through actomyosin networks with longer stress relaxation time scales at high tension. Thus, non-linearity in both the viscous and elastic nature of crosslinked F-actin networks likely plays an important role in regulating the extent and nature of cytoskeletal deformation under different levels of tension.

Acknowledgments

M.L.G. acknowledges support from the Materials Research Science and Engineering Consortium at the University of Chicago, a Packard Fellowship, Burroughs Wellcome Career Award at the Scientific Interface and NIH Director's Pioneer Award.

References

1. Fletcher DA, Mullins RD. Nature. 2010; 463:485–492. [PubMed: 20110992]
2. Stricker J, Falzone T, Gardel ML. J. Biomech. 2010; 43:9–14. [PubMed: 19913792]
3. Alberts, B.; Johnson, A.; Lewis, J.; Raff, M.; Roberts, K.; Walter, P. Molecular Biology of the Cell. 4th edn. Garland Science; 2002.
4. Conti MA, Adelstein RS. J. Cell Sci. 2008; 121:11–18. [PubMed: 18096687]
5. Vicente-Manzanares M, Ma X, Adelstein RS, Horwitz AR. Nat. Rev. Mol. Cell Biol. 2009; 10:778–790. [PubMed: 19851336]
6. MacKintosh FC, Kas J, Janmey PA. Phys. Rev. Lett. 1995; 75:4425–4428. [PubMed: 10059905]
7. Gardel ML, Shin JH, MacKintosh FC, Mahadevan L, Matsudaira P, Weitz DA. Science. 2004; 304:1301–1305. [PubMed: 15166374]
8. Storm C, Pastore JJ, MacKintosh FC, Lubensky TC, Janmey PA. Nature. 2005; 435:191–194. [PubMed: 15889088]
9. Broedersz CP, Kasza KE, Jawerth LM, Muenster S, Weitz DA, MacKintosh FC. Soft Matter. 2010; 6:4120–4127.
10. Lieleg O, Claessens MM, Luan Y, Bausch AR. Phys. Rev. Lett. 2008; 101:108101. [PubMed: 18851260]

11. Lieleg O, Schmoller KM, Claessens MM, Bausch AR. Biophys. J. 2009; 96:4725–4732. [PubMed: 19486695]
12. Tharmann R, Claessens MM, Bausch AR. Phys. Rev. Lett. 2007; 98:088103. [PubMed: 17359131]
13. Wachsstock DH, Schwarz WH, Pollard TD. Biophys. J. 1994; 66:801–809. [PubMed: 8011912]
14. Ward SM, Weins A, Pollak MR, Weitz DA. Biophys. J. 2008; 95:4915–4923. [PubMed: 18689451]
15. Broedersz CP, Depken M, Yao NY, Pollack MR, Weitz DA, MacKintosh FC. Phys. Rev. Lett. 2010; 105:238101. [PubMed: 21231506]
16. Norstrom MF, Smithback PA, Rock RS. J. Biol. Chem. 2010; 285:26326–26334. [PubMed: 20511646]
17. Spudich JA, Watt S. J. Biol. Chem. 1971; 246:4866–4871. [PubMed: 4254541]
18. Kovacs M, Thirumurugan K, Knight PJ, Sellers JR. Proc. Natl. Acad. Sci. U. S. A. 2007; 104:9994–9999. [PubMed: 17548820]
19. Wang F, Kovacs M, Hu A, Limouze J, Harvey EV, Sellers JR. J. Biol. Chem. 2003; 278:27439–27448. [PubMed: 12704189]
20. Guo B, Guilford WH. Proc. Natl. Acad. Sci. U. S. A. 2006; 103:9844–9849. [PubMed: 16785439]
21. Niederman R, Pollard TD. J. Cell Biol. 1975; 67:72–92. [PubMed: 240861]
22. Verkhovsky AB, Svitkina TM, Borisy GG. J. Cell Biol. 1995; 131:989–1002. [PubMed: 7490299]
23. Bendix PM, Koenderink GH, Cuvelier D, Dogic Z, Koeleman BN, Brieher WM, Field CM, Mahadevan L, Weitz DA. Biophys. J. 2008; 94:3126–3136. [PubMed: 18192374]
24. Janmey PA, Peetermans J, Zaner KS, Stossel TP, Tanaka T. J. Biol. Chem. 1986; 261:8357–8362. [PubMed: 3013849]
25. Schmidt CF, Barmann M, Isenberg G, Sackmann E. Macromolecules. 1989; 22:3638.
26. Humphrey D, Duggan C, Saha D, Smith D, Kas J. Nature. 2002; 416:413–416. [PubMed: 11919627]
27. Luan Y, Lieleg O, Wagner B, Bausch AR. Biophys. J. 2008; 94:688–693. [PubMed: 17872953]
28. Rosenfeld SS, Xing J, Chen LQ, Sweeney HL. J. Biol. Chem. 2003; 278:27449–27455. [PubMed: 12740390]
29. Marston SB. Biochem. J. 1982; 203:453–460. [PubMed: 7115298]
30. Vicente-Manzanares M, Zareno J, Whitmore L, Choi CK, Horwitz AF. J. Cell Biol. 2007; 176:573–580. [PubMed: 17312025]
31. Veigel C, Molloy JE, Schmitz S, Kendrick-Jones J. Nat. Cell Biol. 2003; 5:980–986. [PubMed: 14578909]
32. Gardel ML, Schneider IC, Aratyn-Schaus Y, Waterman CM. Annu. Rev. Cell Dev. Biol. 2010; 26:3.1–3.19.
33. Aratyn-Schaus Y, Gardel ML. Curr. Biol. 2010; 20:1145–1153. [PubMed: 20541412]

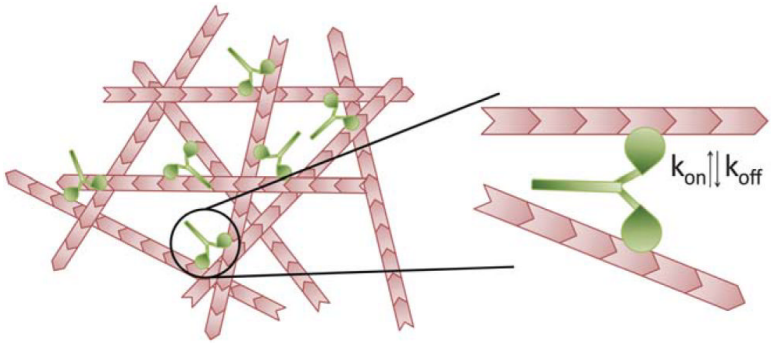

Fig. 1.

Actin network crosslinked by NMMIIB dimers. Actin filaments (pink) are crosslinked by NMMIIB dimers (green). Each dimer has a catalytic head that can bind actin with certain on-rates (k_{on}) and off-rates (k_{off}). The affinity of this bond, k_{off}, is altered by the presence of ATP or ADP.

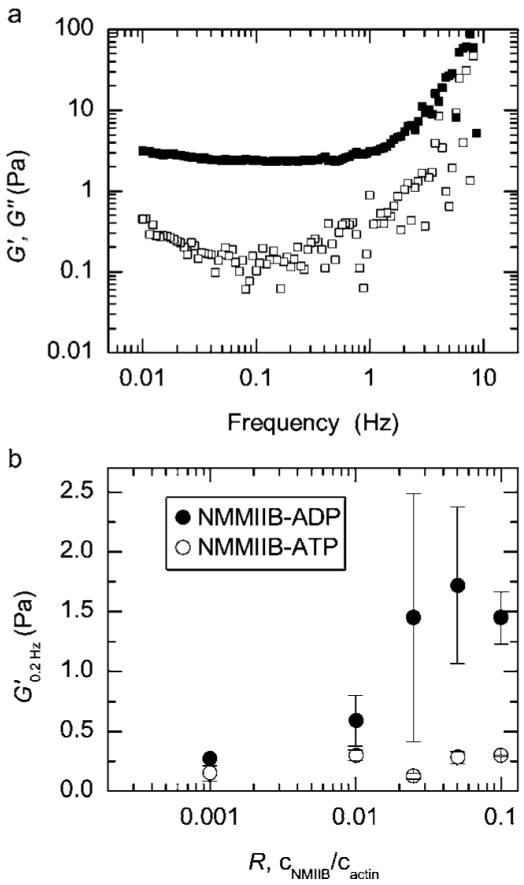

Fig. 2.

NMMIIB crosslinks F-actin in saturating ADP. (a) The frequency dependent linear elastic (closed squares) and viscous (open squares) moduli for actin/NMMIIB–ADP network formed with 10 μM F-actin, 0.5 μM NMMIIB (R = 0.05) in the presence of 2 mM ADP. (b) The elastic modulus measured at 0.2 Hz, $G'_{0.2}$, for actin/NMMIIB networks as R is varied from 0.001 to 0.1. Networks formed in the presence of 2 mM ATP and 2 mM ADP are shown as open and closed circles, respectively. Actin concentration is 10 μM. Error bars are standard error.

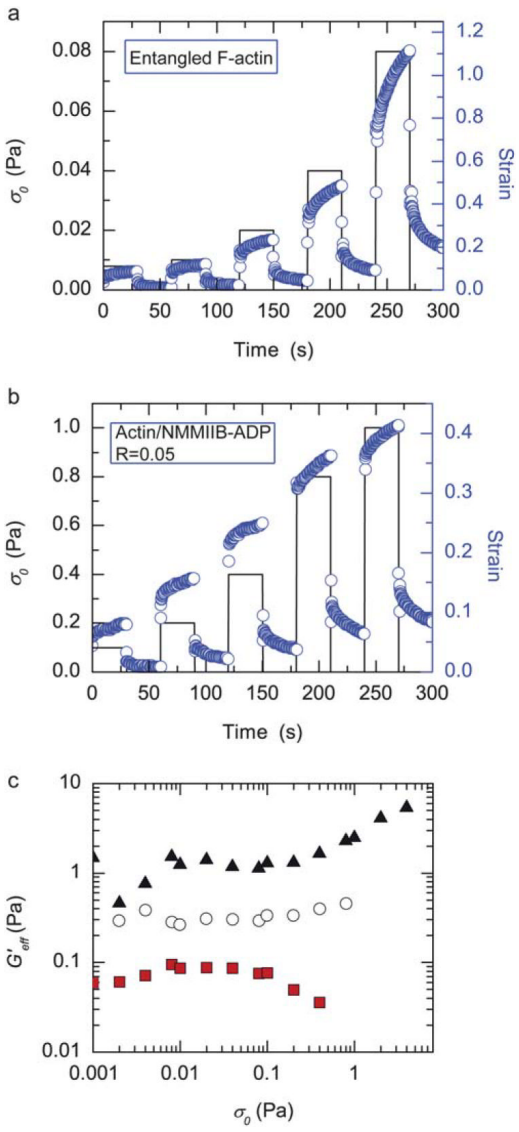

Fig. 3.

Actin/NMMIIB–ADP networks show significant creep and stress stiffen. (a and b) Creep and creep recovery tests lasting 30 s are performed over a range of stresses. The applied stress (solid black line) and resultant strain (open circles, right axis) are shown as a function of experimental time. Data in (a) are of an entangled F-actin solution (c_A = 10 μM) whereas (b) are of a actin/NMMIIB–ADP network (c = 10 μM, R = 0.05) (c) The effective elastic modulus, G'_{eff}, is calculated from the creep tests at different levels of applied stress. Data shown are from an entangled F-actin solution, R = 0, (closed squares) and actin/NMMIIB–ADP networks with R = 0.025 (open circles) or R = 0.05 (closed trian-gles). For all data, c_A = 10 μM.

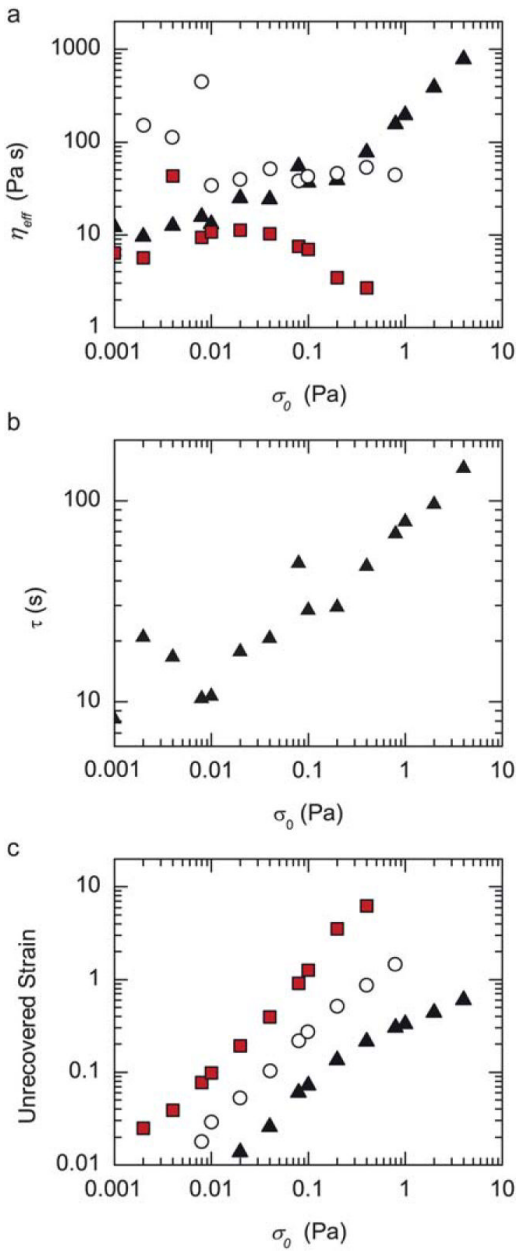

Fig. 4.

Actin/NMMIIB–ADP networks shear thicken. (a) Effective viscosity, η_{eff}, as a function of applied stress, σ_0 for entangled F-actin solution, $R = 0$ (closed squares), and actin/NMMIIB–ADP networks with $R = 0.025$ (open circles) and R = 0.05 (closed triangles). (b) Stress relaxation time scale, τ, as a function of applied stress, σ_0 for actin/NMMIIB–ADP networks with $R = 0.05$. (c) The unrecovered strain after a creep measurement, defined as the difference in the strain prior to a creep measurement and after the recovery phase, as a function of applied stress. Entangled actin solutions (solid squares) and actin/NMMIIB–ADP networks formed with $R = 0.025$ (open circles) and $R = 0.05$ (closed triangles).

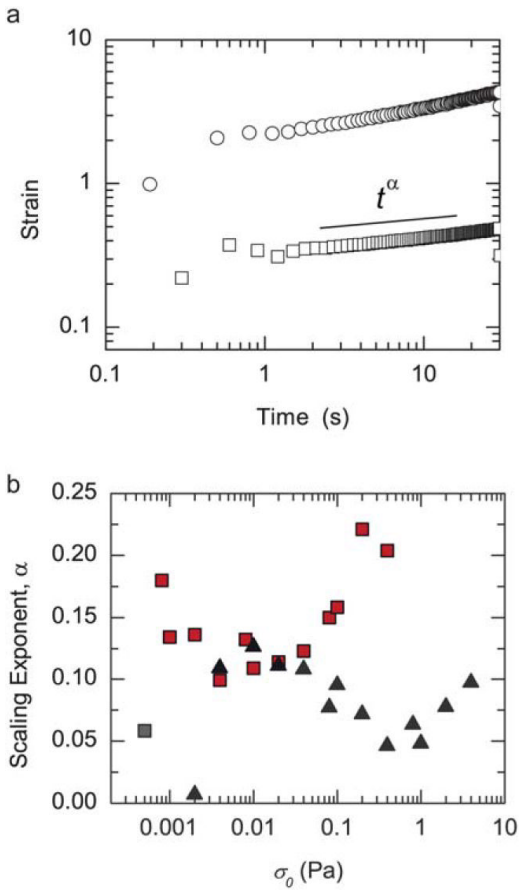

Fig. 5.

Actin/NMMIIB–ADP networks become more solid-like at high stresses. (a) The strain as a function of time for an entangled 10 μM actin solution ($R = 0$) is shown at two applied stresses 0.04 Pa (squares) and 0.2 Pa (circles). A scaling exponent, α, is measured by fitting a power law between 1 and 30 s. (b) The scaling exponent, α, for an actin solution ($R = 0$, squares) and an actin/NMMIIB–ADP network ($R = 0.05$, triangles) as a function of applied stress.